ICARUS **127,** 258–262 (1997)
ARTICLE NO. IS975709

NOTE

Detection of Gaseous Methane on Pluto

LESLIE A. YOUNG[1]

Center for Space Physics, Boston University, Boston, Massachusetts 02215
E-mail: layoung@bu.edu

J. L. ELLIOT[1]

Department of Earth, Atmospheric, and Planetary Sciences and Department of Physics, Massachusetts Institute of Technology, Cambridge, Massachusetts 02139–4307; and Lowell Observatory, 1400 W. Mars Hill Road, Flagstaff, Arizona 86001–4499

ALAN TOKUNAGA[1]

Institute for Astronomy, University of Hawaii, Honolulu, Hawaii 96822

CATHERINE DE BERGH[1]

Observatoire de Paris, 92195 Meudon Cedex, France

AND

TOBIAS OWEN

Institute for Astronomy, University of Hawaii, Honolulu, Hawaii 96822

Received October 10, 1995; revised January 30, 1997

We obtained Pluto's spectrum using the CSHELL echelle spectrograph at NASA's IRTF on Mauna Kea, on 25–26 May 1992, with a spectral resolution of 13,300. The spectral range (5998–6018 cm^{-1}, or 1661.8–1666.9 nm) includes the $R(0)$ and the $Q(1)$–$Q(9)$ lines of the $2\nu_3$ band of methane. The resulting spectrum shows the first detection of gaseous methane on Pluto, with a column height of $1.20^{+3.15}_{-0.87}$ cm-A ($3.22^{+8.46}_{-2.34} \times 10^{19}$ molecule cm^{-2}).

Introduction. This paper presents the first positive detection of gaseous CH_4 in Pluto's atmosphere. Solid CH_4 has been previously identified in Pluto's visible and near-IR spectra at resolutions of a few hundred up to 1200 (e.g., Fink *et al.* 1980; Spencer *et al.* 1990; Owen *et al.* 1993). Unfortunately, these observations cannot be used to find the CH_4 mixing ratio in the atmosphere directly, since the spectra of solid and gaseous CH_4 are essentially indistinguishable at these resolutions. Furthermore, the absorption features due to gaseous CH_4 are hundreds of times weaker than those due to solid CH_4, and have not been detected in these spectra.

Because Pluto's atmosphere is expected to be in vapor-pressure equilibrium with the surface, the surface temperature and composition can be used indirectly to estimate the atmospheric CH_4 mixing ratio (X_{CH4}). Near-IR spectra indicate that Pluto's surface is dominated by frost with 0.5% CO, 1.5% CH_4 (by mass), and N_2 in an intimate mixture (Owen *et al.* 1993). Assuming the N_2–CO–CH_4 frost acts like an ideal mixture, one finds that X_{CH4} is only 0.0001% to 0.001%. However, Lellouch (1994) points out that Triton's X_{CH4} is several hundred times greater than that predicted by the ideal mixture that Cruikshank *et al.* (1993) used to interpret similar spectra of Triton. This can be explained if the N_2–CO–CH_4 frost is nonideal. Lellouch therefore suggests that Pluto's X_{CH4} is inflated by a similar amount, so that $X_{CH4} \approx 0.1\%$. Finally, there is recent spectral evidence of pure CH_4 on Pluto's surface (Schmitt *et al.*, 1994). Pure CH_4 frost would supply more gaseous CH_4 than N_2–CO–CH_4 frost, raising X_{CH4} above the ideal-mixture value.

The thermal structure of Pluto's atmosphere is further evidence that X_{CH4} is larger than the ideal mixture predicts. The temperature of the N_2–CO–CH_4 frost is 40 ± 2 K, from the shape of the N_2 absorption feature at 2148 nm (Tryka *et al.*, 1994), and the brightness temperature of Pluto (which is a global average, including frost-covered and frost-free regions) ranges from 55 K at 60 μm (Sykes *et al.* 1987; Tedesco *et al.* 1987) to 35 K at 1300 μm (Stern *et al.* 1993; Jewitt 1994). In contrast with the cold surface, the atmosphere is 100 K at μbar levels (Elliot and Young 1992), implying a source of heating in the atmosphere. CH_4 can provide the required heating, if $X_{CH4} > 0.1\%$ and there is no CO cooling (Yelle and Lunine 1989). For models that include CO cooling, large enough amounts of gaseous CH_4 can still heat the atmosphere (Lellouch 1994; Strobel *et al.* 1996).

Observations. Both solid and gaseous CH_4 absorb in the near infrared. At sufficiently high spectral resolution, it is possible to distinguish

[1] Visiting observer, Infrared Telescope Facility of Mauna Kea, Hawaii.

0019-1035/97 $25.00

between these two phases because narrow rotation–vibration lines are present only in the gas phase. At 5.5 K, solid CH_4 in an N_2 matrix shows narrow bands, but these bands broaden and coalesce by 20 K (Nelander 1985, Bohn *et al.* 1994), well below Pluto's frost temperature of 40 ± 2 K (Tryka *et al.* 1994).

Using the CSHELL echelle spectrograph (Tokunaga *et al.* 1990; Greene *et al.* 1993) with NASA's Infrared Telescope Facility on Mauna Kea on 25 and 26 May, 1992 (UT), we recorded the spectrum of the Pluto–Charon system from 5998 to 6018 cm^{-1} (1661.8 to 1666.9 nm) at a nominal resolution of 13,300. This spectral range contains the $R(0)$ and $Q(1)$–$Q(9)$ lines of the $2\nu_3$ band of CH_4. Pluto's rotational phase was 0.84 on 25 May (midway between the extremes in Pluto's visible rotational lightcurve) and 0.97 on 26 May (just before the minimum in Pluto's visible rotational lightcurve), where zero phase is defined in Binzel *et al.* (1985), and corresponds to the minimum in the visible lightcurve. Asteroid 532 Herculina and the star 16 Cyg B, a solar analog (Campins *et al.* 1985; Hardorp 1978), were observed to confirm our correction of solar and telluric features. The dispersion was determined from four lines from CSHELL's standard Xe, Kr, and Ar lamps. Because the CSHELL employs a circular-variable filter (CVF) to separate out a single order, the wavelength range is small enough that the wavelength is simply a linear function of detector array column.

Analysis. We extracted the spectra using the optimal extraction algorithm (Horne 1986), as implemented by IRAF's APEXTRACT package (Massey *et al.* 1992). The normalized spectra were combined in weighted means, where the weights were estimated by the scatter in a continuum region. The error in the combined Pluto–Charon spectrum is 7%, based on the propagation of the errors determined for the individual spectra.

At this point, analysis normally proceeds by dividing the object spectra by the standard spectra to remove solar lines, telluric lines, and instrumental effects. However, our standards' doppler shifts were different from Pluto's, so the solar lines would not have divided correctly. Instead, we chose to model the Pluto and standard spectra.

The steps in our model of the Pluto–Charon spectrum mimic the physical steps that yield the observed spectrum. Sunlight is absorbed by CH_4 in Pluto's atmosphere, reflected from the surface, and absorbed again as it leaves Pluto's atmosphere; it is simply reflected from Charon's surface. These two components of reflected sunlight then pass through the Earth's atmosphere, and are absorbed by H_2O and CH_4. Internal reflections in the CVF create an interference pattern (''fringing''), which causes a low-order undulation in the continuum. Finally, the spectrum is convolved by the slit function as it passes through the instrument (convolution is represented by the symbol $\otimes$). Putting these all together, the observed normalized spectrum is

$$M(i) = F(i)G(\lambda) \otimes [T(\lambda)\, S(\lambda)\, \{C + (1 - C)\, P(\lambda)\}], \qquad (1)$$

where F is the fringing as a function of pixel i, G is the slit function, which is approximated by a Gaussian, T is the telluric absorption, S is the solar spectrum, C is the ratio of Charon's flux to the flux from both Pluto and Charon in the continuum (constant with wavelength), and P is the absorption due to Pluto's atmosphere. T, S, C, and P are between 0 and 1.

Pluto's CH_4 absorption was calculated on a line-by-line basis, using the 65 lines in the HITRAN database (Rothman *et al.* 1992) that fell within our spectral range, including one weak line from $^{13}CH_4$. The strongest of these lines are the $R(0)$ and the $Q(1)$–$Q(9)$ lines of the $2\nu_3$ band of CH_4. We did not include H_2O, CO, or CO_2, whose lines in this region are 100–1000 times weaker than the CH_4 lines. No other molecules from the HITRAN database had lines listed in this region, including N_2, C_2H_2, or C_2H_6.

At Pluto's low pressures, the line shape is the Doppler line shape. Because this is pressure independent, an isothermal atmosphere can be modeled as a single-layer atmosphere. We used a temperature of 100 K, the temperature derived from the stellar occultation for a predominately N_2 atmosphere (Elliot and Young 1992). The relationship between P and the vertical optical depth, τ, depends on the limb darkening. Pluto has no detectable limb darkening at 0.55 μm (Young and Binzel 1994), so we assume no limb darkening at these wavelengths as well. In this case, $P = 2\ E_3(2\tau)$, where E_3 is the exponential integral. For small τ, this reduces to $P \approx 1 - 4\ \tau \approx \exp(-4\tau)$, reproducing the familiar airmass factor of 4. Because only H_2O has been detected on Charon (e.g., Buie *et al.* 1987), and H_2O is nonvolatile in the outer solar system, we assume that Charon has no gaseous absorption.

The spectra of solid H_2O and CH_4, and therefore the reflectance of the surfaces of Pluto and Charon, do not vary with wavelength over our small spectral range. In particular, the ratio of Charon's flux to the combined and unattenuated Pluto–Charon flux (C in Eq. (1)) is constant with wavelength. At a rotational phase of 0.75, Charon contributes 15% of the combined Pluto–Charon flux at 1622–1712 nm (through a CVF with a bandpass of 90 nm; Buie *et al.* 1987). The combined flux varies with wavelength throughout 1622–1712 nm; the combined flux at our wavelength is 62–75% of the combined flux through 1622–1712 nm, and depends on rotational phase (Owen *et al.* 1993; Ted Roush, personal communication). We assumed that Charon's contribution, C, ranged from 0.15/0.62 to 0.15/0.75, or 20%–24% of the combined flux.

It is vital in this analysis to distinguish between CH_4 absorption from Earth's and from Pluto's atmosphere. The telluric absorption was modeled with the ATRAN program (Lord 1992), which can calculate atmospheric transmission for any altitude, airmass, wavelength, resolution, and concentration of H_2O, CH_4, and other species. Although telluric H_2O can vary considerably during the night, changing the precipitable H_2O from 1 to 3 mm changed the absorption by an insignificant 1%; we assumed 3 mm H_2O throughout. In one study, telluric CH_4 was found to have a daily variation of only about 0.1% (Khalil *et al.* 1993), so CH_4 was essentially constant during the two-night run. Therefore, we assumed that the telluric absorption did not vary over the observing run. The mean airmass for each object was the weighted mean of the airmasses of the individual spectra. Pluto spanned 1.1 to 2.3 airmasses, with a weighted mean airmass of 1.25—close to the unweighted mean airmass of 1.29.

The solar spectrum was provided by the KPNO Solar Atlas (Livingston and Wallace 1991). The fringing is well modeled by the first seven parameters in a Fourier series (a constant and three sine–cosine pairs). The nominal dispersion and slit function were determined from CSHELL's standard lamps. At 1.5 arcsec (6 pixels), our slit was wider than the typical seeing disk, so the position and angular size of the star also contributed to the ''slit'' function and dispersion. For instance, a seeing disk of 1 arcsec yields an effective resolution of 20,000, and a drift of 0.5 arcsec in the star's position would offset the wavelengths by 2 columns. An error in the tabulated value for 16 Cyg B's radial velocity (Wilson 1953) would produce a similar shift.

We used the standards (532 Herculina and the star 16 Cyg B) to confirm our modeling of the solar and telluric lines and to measure the amount of telluric CH_4. In fitting the standard spectra, we allowed the strength and width of the solar lines, the amount of telluric CH_4, the width of the slit function, and the dispersion to be free parameters. We found that the ATRAN program correctly calculated the amount of absorption by telluric CH_4, without modification. Absorption by telluric H_2O occurred primarily at 1663.4–1663.5 nm, which we exclude from the analysis. There are no other important absorbers in the Earth's atmosphere at these wavelengths. The solar lines we observed in the standards are broader than the solar lines from the KPNO atlas, perhaps because the observations for the KPNO atlas were of the center of the solar disk, while we observed disk-integrated spectra. The strengths of the solar lines in the KPNO atlas matched the asteroid, as expected, since the asteroid reflects the solar spectrum. The solar line strengths had to be increased to match

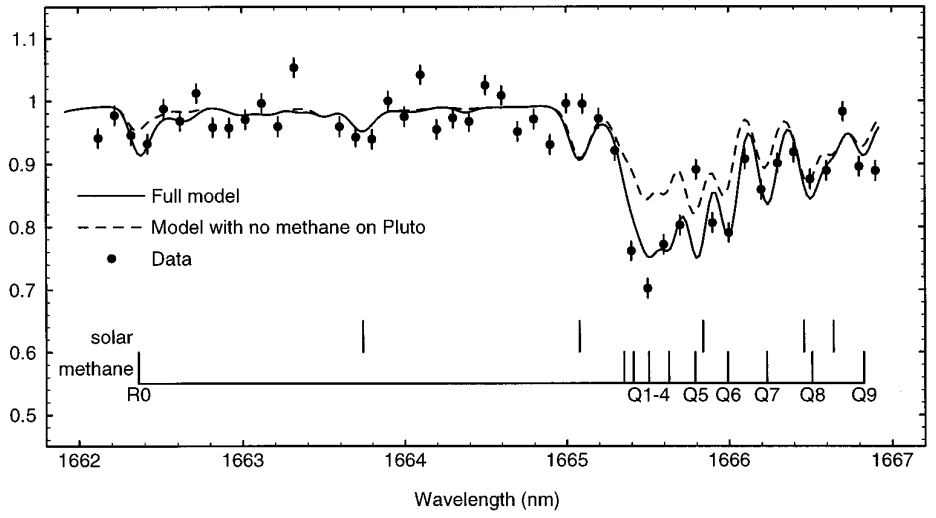

FIG. 1. Pluto data and models. The upper, dashed curve is the product of the solar spectrum and telluric absorption for Pluto's mean airmass of 1.25. The lower, solid curve is the product of the above spectrum and absorption by Pluto's atmospheric methane at a temperature of 100 K and a column height of 1.20 cm-A (plus a 22% contribution from Charon, see Eq. (1)). The points represent the observed spectrum of the Pluto–Charon system. The data have been corrected for the low-order interference fringing, and every five points have been averaged. The important lines in the solar spectrum, and the observed rotation lines in the $2\nu_3$ band of CH_4, are indicated below the models. These lines are red-shifted by 0.04 nm relative to telluric CH_4 because of Pluto's motion.

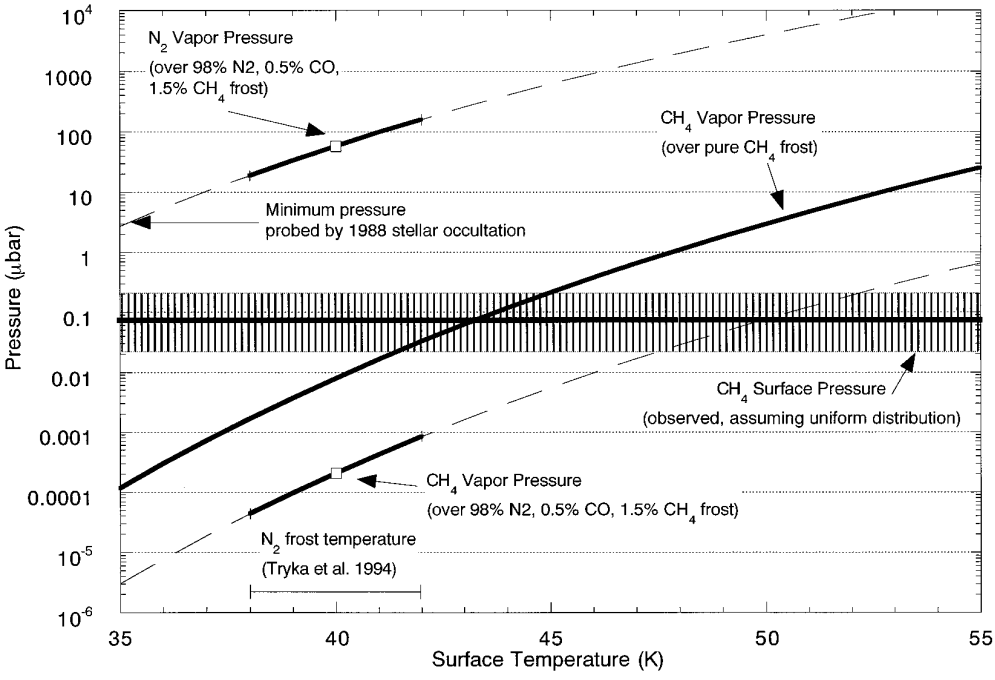

FIG. 2. Surface pressures. The horizontal line is the observed partial pressure of CH_4 at the surface, if the CH_4 mixing ratio is constant with altitude. If CH_4 were concentrated in the lower atmosphere, the implied surface pressure would be higher. The upper curve is the vapor pressure of N_2 over an intimate mixture of 98% N_2, 0.5% CO, and 1.5% CH_4 (by mass), and should be close to the total atmospheric surface pressure. The lower curve is the vapor pressure of CH_4 over the same mixture. The solid portions on the upper and lower curves show the pressures for a frost temperature of 40 ± 2 K. The middle curve is the vapor pressure of pure CH_4. The upper curve shows that CH_4 is a minor constituent, with a vertically averaged abundance of ~0.1%. If the CH_4 is evenly distributed vertically, it is oversaturated with respect to the N_2–CO–CH_4 mixture by a factor of several hundred, but in equilibrium with pure CH_4 at 41–45 K.

the solar analog, but we attributed this to differences between the spectra of 16 Cyg B and the sun, rather than a problem with the KPNO atlas.

In contrast to the standard spectra, the Pluto–Charon spectrum cannot be explained solely by telluric and solar features. The spectrum consisting only of reflected sunlight and telluric absorption at Pluto's airmass of 1.25 is the upper, dashed line in Fig. 1. The normalized Pluto–Charon spectrum, binned to 1-nm resolution, is shown as points in Fig. 1. The spectrum shows absorption features at 1665.4–1662.2 nm that are deeper than can be accounted for by the reflected solar spectrum and telluric absorption. To investigate the possibility that this excess absorption was due to an underestimate of Pluto's airmass, we asked what airmass would be needed to produce these features. The resulting effective airmass, 2.05 $\pm$ 0.37, was more than 2σ larger than the actual airmass of the observations.

Since we could accurately model the telluric absorptions and solar lines seen in the standards, we applied these models to Pluto as well. Holding the strength of the solar lines and the amount of telluric CH_4 fixed, we fit Eq. (1) to the Pluto–Charon spectrum in a least squares sense. We first performed a parameter-space search and investigated χ^2 (the sum of weighted, squared residuals) as a function of column height, ξ. From the χ^2 for no absorption, we calculated that there is less than a 1% chance that the features longward of 1665 nm are caused by random noise (Press *et al*. 1988). We find that χ^2 is a parabolic function of $\ln(\xi)$, not ξ, so we use $\ln(\xi)$ as the free parameter. This leads to unequal error bars in ξ. The best-fit CH_4 column height was $1.20^{+3.15}_{-0.87}$ cm-A ($3.22^{+8.46}_{-2.34} \times 10^{19}$ cm^{-2}) for a temperature of 100 K, where we give the 1σ errors. The model spectrum is shown as a solid line in Fig. 1. The difference between the dashed and solid lines is due to absorption by Pluto's gaseous CH_4.

Discussion. Our detection of $1.20^{+3.15}_{-0.87}$ cm-A of CH_4 confirms that CH_4 is only a minor constituent in Pluto's atmosphere, as expected from the dominance of N_2 on the surface (Owen *et al*. 1993), since a pure CH_4 atmosphere would need a column height greater than 23.9 cm-A to explain the 1988 stellar occultation (Elliot and Young 1992). If Pluto's atmosphere had significant scattering by haze, the effective path length would be longer, so that the same absorption could be achieved with less CH_4. Therefore, for a scattering atmosphere, these observations imply an even smaller CH_4 column abundance.

The partial pressure of CH_4 at the surface would be $0.072^{+0.189}_{-0.052}$ μbar if the CH_4 were evenly distributed in an N_2 atmosphere. This pressure is indicated by the horizontal line in Fig. 2, with the hashed area representing the 1σ error. However, this analysis does not provide information on CH_4's vertical distribution. For example, if CH_4 were confined below a certain altitude because of photochemical reactions, then the partial pressure of CH_4 at the surface implied by this analysis would be increased.

To find the mean CH_4 mixing ratio, we need to estimate the total atmospheric number density, or, equivalently, the total surface pressure. If the atmosphere is mostly N_2 and in vapor-pressure equilibrium with N_2 frost, then the surface pressure will be $V(T)_{N2}$, the vapor pressure of N_2 at the surface temperature. The N_2 vapor-pressure curve is indicated in Fig. 2 by the uppermost curved line (Brown and Ziegler 1980). The 1988 stellar occultation probed down to a pressure of at least 3.25 μbar (Elliot and Young 1992), as indicated by the arrow at 35.25 K. The solid portion of the line reflects the vapor pressure of N_2 at the observed N_2 frost temperature of 40 $\pm$ 2 K (Tryka *et al*. 1994). For a N_2 frost temperature of 40 K, the N_2 surface pressure is 58 μbar. This pressure implies a deep Pluto atmosphere, as first proposed by Stansberry *et al.* (1994) and investigated for a range of atmospheric structures by Young (1994). Briefly, the pressure at 1215 $\pm$ 11 km is 2.38 $\pm$ 0.49 μbar (Elliot & Young 1992), or 3.2 scale heights above a 58 μbar surface. Since the scale height below the occultation levels is at least 20 km, a 40 K surface must lie below 1162 km.

For an N_2 surface pressure of 58 μbar, the mean gaseous CH_4 mixing ratio is 0.03–0.45%. According to atmospheric models, 0.1% CH_4 is enough to heat the middle atmosphere in the absence of CO cooling (Yelle and Lunine 1989), but is far less than the 10% needed to raise the temperature in the presence of CO cooling or to reproduce the "kink" in the occultation lightcurve by refraction alone (Lellouch 1994; Hubbard *et al.* 1990; Strobel *et al.* 1996).

The mean gaseous CH_4 mixing ratio is several hundred times larger than predicted by an ideal mixture of N_2–CO–CH_4, on Pluto as well as on Triton. Assuming Raoult's law, the vapor pressure of CH_4 over an ideal mixture of 98% N_2, 0.5% CO, and 1.5% CH_4 (by mass) is 38 times lower than the vapor pressure over pure CH_4. The lowest curve plotted in Fig. 2 is the vapor pressure of CH_4 over the N_2–CO–CH_4 intimate mixture. Since the CH_4 that is mixed with N_2 should have the same temperature as the N_2, the range of 40 $\pm$ 2 K is indicated by a solid line on this curve as well. For a surface at 40 K, the partial pressure of CH_4 (assuming the gaseous CH_4 mixing ratio is constant with altitude) is 360 times higher than the vapor pressure of CH_4 over the N_2-CO-CH_4 intimate mixture.

A partial pressure of $0.072^{+0.189}_{-0.052}$ μbar is consistent with CH_4 in vapor-pressure equilibrium over pure CH_4 at 41–45 K, as indicated by the middle curve in Fig. 2. Thus, the overabundance of gaseous CH_4 relative to the ideal mixture lends weight to the tentative identification of pure CH_4 on Pluto's surface (Schmitt *et al.* 1994).

ACKNOWLEDGMENTS

Steven Lord provided the ATRAN program and much useful discussion on how to calculate spectra. Laurence S. Rothman provided the HITRAN data base on CD-ROM. Bobby Bus and Richard Freedman gave invaluable help. The NSO/Kitt Peak FTS data used here were produced by NSF/NOAO. This work was supported, in part, by NASA Grant NAGW-3296. This work was completed while L. Young held a National Research Council–NASA Ames Research Associateship.

REFERENCES

Binzel, R. P., D. J. Tholen, E. F. Tedesco, B. J. Buratti, and R. M. Nelson 1985. The detection of eclipses in the Pluto–Charon system. *Science* **228**, 1193–1195.

Bohn, R. B., S. A. Sandford, L. J. Allamandola, and D. P. Cruikshank 1994. Infrared spectroscopy of Triton and Pluto ice analogs: The case for saturated hydrocarbons. *Icarus* **111**, 151–173.

Brown, G. N., Jr., and W. T. Ziegler 1980. Vapor pressure and heats of vaporization and sublimation of liquids and solids of interest in cryogenics below 1-atm pressure. *Adv. Cryog. Eng.* **25**, 662–670.

Buie, M. W., D. P. Cruikshank, L. A. Lebofsky, and E. F. Tedesco 1987. Water frost on Charon. *Nature* **329**, 522–523.

Campins, H., G. H. Rieke, and M. J. Lebofsky 1985. Absolute calibration of photometry at 1 through 5 μm. *Astron. J.* **90**, 896–899.

Cruikshank, D. P., T. L. Roush, T. C. Owen, T. R. Geballe, C. de Bergh, B. Schmitt, R. H. Brown, and M. J. Bartholomew 1993. Ices on the surface of Triton. *Science* **261**, 742–745.

Elliot, J. L., and L. A. Young 1992. Analysis of stellar occultation data for planetary atmospheres. I. Model fitting, with application to Pluto. *Astron. J.* **103**, 991–1015.

Fink, U., B. A. Smith, D. C. Benner, J. R. Johnson, H. J. Reitsema, and J. A. Westphal 1980. Detection of a CH_4 atmosphere on Pluto. *Icarus* **44**, 62–71.

Greene, T. P., A. T. Tokunaga, D. W. Toomey, and J. S. Carr 1993. CSHELL: A high-resolution 1–5 micron cryogenic echelle spectrograph for the IRTF. *Proc. SPIE* **1946**, 313–324.

Hardorp, J. 1978. The Sun among the stars. I. A search for solar spectral analogs. *Astron. Astrophys.* **63**, 383–390.

HORNE, K. 1986. An optimal extraction algorithm for CCD spectroscopy. *Publ. Astron. Soc. Pacific* **98**, 609–617.

HUBBARD, W. B., R. V. YELLE, AND J. I. LUNINE 1990. Nonisothermal Pluto atmosphere models. *Icarus* **84**, 1–11.

JEWITT, D. C. 1994. Heat from Pluto. *Astron. J.* **107**, 372–378.

KHALIL, M. A. K., R. A. RASMUSSEN, AND F. MORAES 1993. Atmospheric methane at Cape Meares: Analysis of a high-resolution data base and its environmental implications. *J. Geophys. Res.* **98**, 14,753–14,770.

LELLOUCH, E. 1994. The thermal structure of Pluto's atmosphere: Clear vs hazy models. *Icarus* **108**, 255–264.

LIVINGSTON, W., AND L. WALLACE 1991. *An Atlas of the Solar Spectrum in the Infrared from 1850 to 9000 cm*$^{-1}$ (1.1 to 5.4 Microns). NSO Technical Report #91–001, National Solar Observatory, NOAO, Tucson.

LORD, S. D. 1992. *A New Software Tool for Computing Earth's Atmospheric Transmission of Near- and Far-Infrared Radiation*. NASA TM-103957, Ames Research Center.

NELANDER, B. 1985. An infrared study of the rotation of methane in solid nitrogen. *J. Chem. Phys*. **82**, 5340–5345.

MASSEY, P., F. VALDES, AND J. BARNES 1992. *A User's Guide to Reducing Slit Spectra with IRAF*. NOAO/CCS.

OWEN, T. C., T. L. ROUSH, D. P. CRUIKSHANK, J. L. ELLIOT, L. A. YOUNG, C. DE BERGH, B. SCHMITT, T. R. GEBALLE, R. H. BROWN, AND M. J. BARTHOLOMEW 1993. Surface ices and the atmospheric composition of Pluto. *Science* **261**, 745–748.

PRESS, W. H., B. P. FLANNERY, S. A. TEUKOLSKY, AND W. T. VETTERLING 1988. *Numerical Recipes in C.* Cambridge Univ. Press, Cambridge, UK.

SCHMITT, B., S. DOUTÉ, E. QUIRICO, A. BENCHKOURA, C. DE BERGH, T. C. OWEN, AND D. P. CRUIKSHANK 1994. The state and composition of the surface of Pluto: Laboratory experiments and numerical modeling. *Bull. Am. Astron. Soc.* **26**, 1170.

SPENCER, J. R., M. W. BUIE, AND G. L. BJORAKER 1990. Solid methane on Triton and Pluto: 3- to 4-μm spectrophotometry. *Icarus* **88**, 491–496.

STANSBERRY, J. A., J. I. LUNINE, W. B. HUBBARD, R. V. YELLE, AND D. M. HUNTEN 1994. Mirages and the nature of Pluto's atmosphere. *Icarus* **111**, 503–513.

STERN, S. A., D. A. WEINTRAUB, AND M. C. FESTOU 1993. Evidence for a low surface temperature on Pluto from millimeter-wave thermal emission measurements. *Science* **261**, 1713–1716.

STROBEL, D. F., X. ZHU, M. E. SUMMERS, AND M. H. STEVENS 1996. On the vertical thermal structure of Pluto's atmosphere. *Icarus* **120**, 266–289.

SYKES, M. V., R. M. CUTRI, L. A. LEBOFSKY, AND R. P. BINZEL 1987. IRAS serendipitous survey observations of Pluto and Charon. *Science* **237**, 1336–1340.

ROTHMAN, L. S., R. R. GAMACHE, R. H. TIPPING, C. P. RINSLAND, M. A. H. SMITH, D. C. BENNER, V. M. DEVI, J. M. FLAUD, C. CAMY-PEYRET, A. PERRIN, A. GOLDMAN, S. T. MASSIE, L. R. BROWN, AND R. A. TOTH 1992. The HITRAN molecular database: Editions of 1991 and 1992. *J. Quant. Spectrosc. Radiat. Transfer* **48**, 469–507.

TEDESCO, E. F., G. J. VEEDER, JR., R. S. DUNBAR, AND L. A. LEBOFSKY 1987. IRAS constraints on the sizes of Pluto and Charon. *Nature* **327**, 127–129.

TOKUNAGA, A. T., D. W. TOOMEY, J. CARR, D. N. B. HALL, AND H. W. EPPS 1990. Design for a 1–5 μm cryogenic echelle spectrograph for the NASA IRTF. *Proc. SPIE* **1235**, 131–143.

TRYKA, K. A., R. H. BROWN, D. P. CRUIKSHANK, AND T. C. OWEN 1994. The temperature of nitrogen ice on Pluto and its implications for flux measurements. *Icarus* **112**, 513–527.

WILSON, R. E. 1953. *General Catalog of Stellar Radial Velocities.* Carnegie Institution of Washington, Washington, DC.

YELLE, R. V., AND J. I. LUNINE 1989. Evidence for a molecule heavier than methane in the atmosphere of Pluto. *Nature* **339**, 288–290.

YOUNG, L. A. 1994. *Bulk Properties and Atmospheric Structure of Pluto and Charon.* Ph. D. Thesis, Massachusetts Institute of Technology.

YOUNG, E., AND R. BINZEL 1994. A new determination of radii and limb parameters for Pluto and Charon from mutual event lightcurves. *Icarus* **108**, 219–224.